Journal of
Marine Science and Engineering

Article

Experimental Study on the Effects of Waves and Current on Ice Melting

Tianyi He [1], Huijie Hu [1], Ding Tang [1], Xu Chen [1], Jing Meng [1], Yong Cao [1,*] and Xianqing Lv [1,2]

[1] College of Oceanic and Atmospheric Sciences, Ocean University of China, Qingdao 266100, China; hty2942@stu.ouc.edu.cn (T.H.); huhuijie1105@stu.ouc.edu.cn (H.H.); td2585@stu.ouc.edu.cn (D.T.); chenxu001@ouc.edu.cn (X.C.); mengjing@ouc.edu.cn (J.M.); xqinglv@ouc.edu.cn (X.L.)
[2] Physical Oceanography Laboratory/CIMST, Ocean University of China, Qingdao 266100, China
* Correspondence: caoyong@ouc.edu.cn

Abstract: Ice melting plays a crucial role in ocean circulation and global climate. Laboratory experiments were used to study the dynamic mechanisms of the influence of waves and currents on ice melting. The results showed that under near stable air temperature and water temperature conditions, the ice melting rate was significantly greater with waves than that without waves, as well as the higher the wave height, the greater the melting rate. This is related to the increase in the contact area between ice and water by waves. Further research was carried out to observe the flow field at different locations on the ice bottom, ice sides, and behind the ice by particle image velocimetry (PIV) and dyeing experiments. At different flow velocities, the changes in the side melting rate and bottom melting rate were not the same. Meltwater is attached to the bottom in the form of plume at low background flow velocity, which leads to the slowness of the heat exchange between the ice with a higher ambient temperature. Therefore, the melting of the ice bottom and the ice side were slower at low flow velocity. At high background flow velocity, there is strong shear instability and vortex at the ice bottom and behind the ice. The dissipation and mixing effects caused by vortices accelerate the melting of the ice bottom and the ice back. The thermodynamic factors, such as air temperature and water temperature, had significant impacts in the experiments. Further research needs to improve the accuracy of temperature control of experimental equipment. Computational fluid dynamics and sensitive tests of numerical simulation may also be carried out on ice melting.

Keywords: ice; current; wave; melting rate; experiment

check for updates

Citation: He, T.; Hu, H.; Tang, D.; Chen, X.; Meng, J.; Cao, Y.; Lv, X. Experimental Study on the Effects of Waves and Current on Ice Melting. *J. Mar. Sci. Eng.* **2023**, *11*, 1209. https://doi.org/10.3390/jmse11061209

Academic Editor: Sasan Tavakoli

Received: 12 May 2023
Revised: 5 June 2023
Accepted: 9 June 2023
Published: 10 June 2023

1. Introduction

The mass loss of ice from the North and South Poles has increased compared to the past decade [1]. Half of this mass loss can be attributed to the cracking of ice shelves and icebergs, particularly those at the edges of the Antarctic and Greenland. As these fractured icebergs float with ocean currents, they gradually melt and release fresh-water into the surrounding ocean. This process can affect ocean circulation, biological activities, and sea ice formation. There are two main components of mass loss from icebergs, melting above the air–sea interface and melting below the sea surface [2,3]. Solar radiation and wind can cause forced convection and sublimation above the air–sea interface, but this process can be ignored in comparison to the wave erosion process at this interface. The wave erosion process can both transfer heat and break the iceberg. Below the air–sea interface, buoyancy and forced convection play important roles in melting. Melting caused by forced convection is a function of the external fluid (e.g., velocity, temperature, and salinity) and the physical properties of the ice (e.g., temperature).

In order to understand the physical processes and account for underwater melting in general circulation models (GCMs), parameterization schemes have been proposed [4,5] to predict the large-scale distribution of meltwater along modeled iceberg trajectories [6].

However, these schemes can be overly simplified. For example, Stern et al. [7] showed that the current scheme is not applicable to flat ice, and some numerical models neglect the effects of iceberg melting plumes by calculating side melt using entirely velocity-independent side melt rates [8]. Furthermore, hydrographic surveys have shown that iceberg melting plumes can enhance upwelling and cool temperatures [9–11]. To improve parameterization schemes for underwater iceberg melting, especially considering melting plume effects, the dynamic mechanisms of iceberg melting have been studied under laboratory conditions. These studies have investigated the influence of vertical temperature and salinity gradients on the melting rate, shape evolution of melting ice, and the distribution of meltwater assuming no background flow [12–15]. Buoyancy meltwater generates side melting, and the distribution of melting water is either in the surface layer or the iceberg draft under different speeds of background flow [16]. In addition, icebergs calving into Greenlandic Fjords frequently experience strongly sheared flows over their draft, which can lead to a nonlinear increase in the side melting rate of the icebergs [17]. The strong shear flow not only affects sea ice, but also has a significant impact on the shore foundation. Therefore, the study of shear stress can refer to other experimental studies [18,19]. However, the factors that influence the distribution of iceberg melting plumes under different speeds of background flow are still not well understood.

Limited research has been conducted on the specific mechanisms of how waves impact sea ice melting [20]. Sea ice can become fatigued under periodic pressure, causing it to rupture and break at stresses much lower than its bending strength [21]. Observations of the Antarctic sea ice edge from 1997 to 2009 have shown that an increase in effective wave height is correlated with increased sea ice fracturing and retreat [22]. However, there is a lack of laboratory research on how waves promote the melting of floating ice. Conducting laboratory research on the impact of waves on floating ice melting by control variables such as room temperature, water temperature, and wave height, increase the accuracy of measured data and provide a theoretical basis for future research on the mechanisms of how waves affect sea ice melting.

The goal of this study was to compare the differences in ice melting under distinct wave conditions and homogeneous flow velocity in the laboratory. By exploring the physical dynamics of melting plume behavior, we can gain a better understanding of ice-flow interactions and improve iceberg parameterization. This information can be used to inform future research on the impact of waves on sea ice melting and further our understanding of this important area of study in oceanography.

2. Experiments

2.1. Instrument

The experiments included the melting processes under the action of distinct waves and currents, respectively.

(1) Experiment on the effect of waves on sea ice melting

This experiment was conducted in an experimental tank at the Physics Ocean Thermostatic Laboratory of Ocean University of China, simulating the conditions in the Polar region and keeping the room temperature below 0 °C. The experimental study of the effect of waves on iceberg melting was carried out in a recirculating flume of width 20 cm, length 150 cm, and depth 20 cm (Figure 1). Different wave heights were produced using a wave machine, and the frequency of the waves used during the experiment was recorded.

The following twelve experiments (shown in Table 1) were conducted to measure the effects of water temperature, ambient temperature, and wave height on sea ice melting. In the first five experiments, the initial side and bottom area of each ice block were measured before being submerged in water. Measurements were taken again after ten minutes, with the second group serving as a control group without waves. The first and fourth groups had the same water temperature, but the room temperature in the fourth group was 3 °C lower than that in the first group. The room temperature was the same in the fourth and fifth groups, but the water temperature in the fifth group was 1.4 °C lower than that in the fourth group. The wave height in the third group was significantly lower than the other three groups with waves.

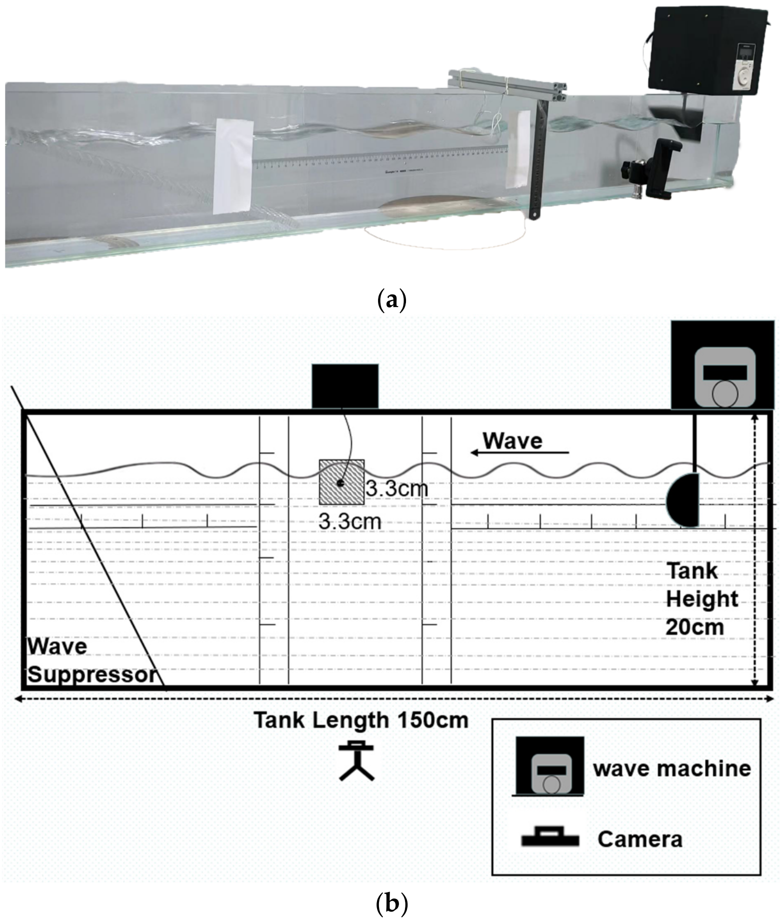

Figure 1. Photograph (**a**) and diagram (**b**) of wave experimental device (side view).

Table 1. Experimental setup groups of the effect of wave on iceberg melting.

	Wave Height (cm)	Wave Length (cm)	Period (s)	Room Temperature (°C)	Water Temperature (°C)
1	2.00	17.5	0.32	0.4	2.4
2	0.00	0.0	0.00	0.4	2.4
3	1.45	18.4	0.32	0.0	1.5
4	2.70	18.7	0.33	−2.6	2.4
5	2.26	19.0	0.32	−2.6	1.0
6	2.30	20.0	0.33	2.4	2.2
7	0.00	0.0	0.00	2.4	2.2
8	0.55	16.0	0.60	3.5	2.5
9	0.00	0.0	0.00	3.5	2.5
10	3.20	18.6	0.33	1.3	2.4
11	0.00	0.0	0.00	1.3	2.4
12	1.20	16.6	0.54	3.0	3.3

In the seven subsequent experiments, the ice mass, ambient temperature, and water temperature were measured every three minutes. The seventh, ninth, and eleventh groups served as control groups without waves for the sixth, eighth, and tenth groups, respectively.

(2) Experiment on the effect of current on ice melting

The experiment of ice melting under distinct flow velocity was carried out in a recirculating flume with a width 20 cm, length 136.5 cm, and depth 30 cm, independently designed and developed by Ocean University of China, as shown in Figure 2. Compared with the electric pump type tank, the recirculating flume has the advantages of stable and easy adjustment of the flow velocity. It can produce a uniform background flow. Fresh ice that was 18 cm length, 10 cm width and 12 cm height was frozen in each experiment. The ice was fixed in the homogenous background flow with the velocity of 0.02 m/s, 0.025 m/s, 0.03 m/s, 0.035 m/s, 0.04 m/s, 0.045 m/s, 0.05 m/s, and 0.055 m/s, respectively, for 8 groups of experiments. During each experiment, the mass of the ice was measured over a period dT = 3 min, and so were the changes of the side area and bottom area of the ice. The temperatures of ice and water were recorded with a temperature probe every 10 s.

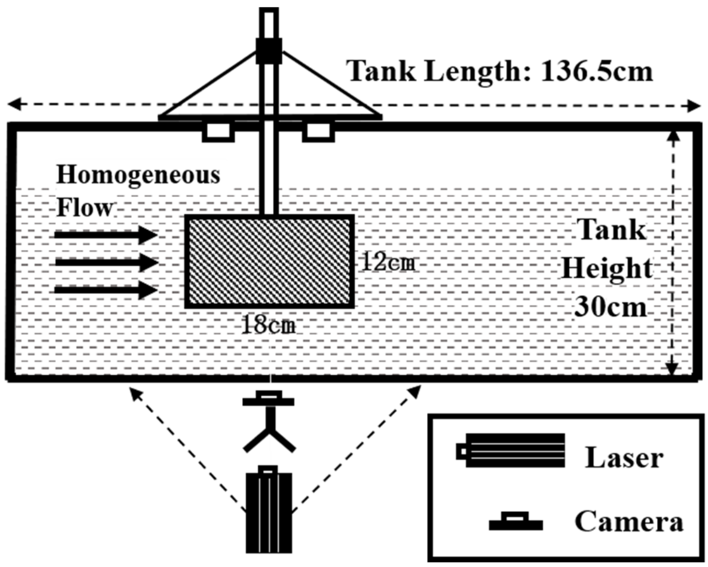

(a)

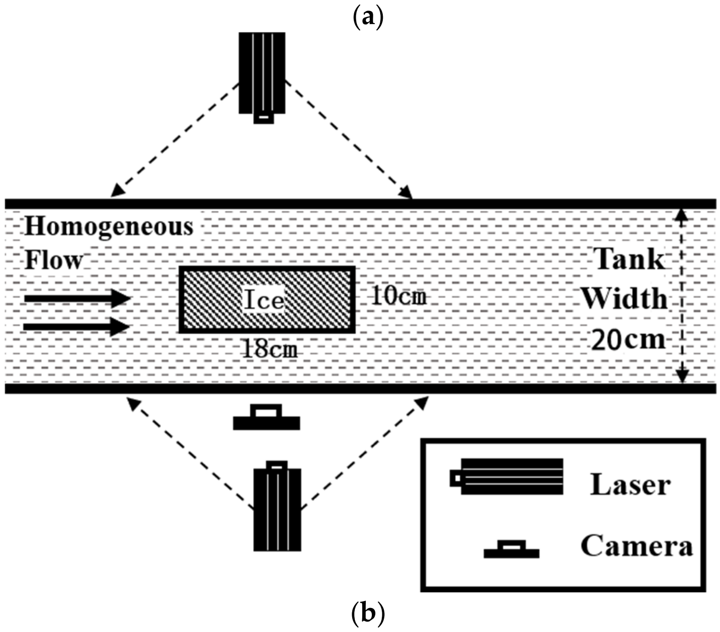

(b)

Figure 2. Diagram of current experimental device (**a**) side view; (**b**) bottom view.

2.2. Data Acquisition

Particle image velocimetry (PIV) is widely used in experimental fluid mechanics [23–26] to measure the instantaneous velocity field of a flow with high spatial and temporal resolution. PIV measurements are most commonly snapshots of the two- or three-component velocity vector field on a planar cross-section of the flow, but in recent years new developments have made it possible to measure the velocity over volumetric domains and to measure sequences of velocity in time at rates sufficient to resolve the temporal evolution [27].

The interaction between ice melting and flow at distinct flow velocities was studied by the PIV system which was used to measure the flow distribution at the ice bottom and the back of ice in the direction of flow. The PIV system is shown in Figure 1. The sheet light source was a pulsed dye laser with wavelength 532 nm and power 4 W, which was vertically irradiated upward from the ice bottom. The tracing particles with 50 μM were used to display the change of the flow field. The frame rate of the camera was 40 Hz, and the main area is (40 × 40) pix, sub-area was (20 × 20) pix.

3. Methods of Calculation

The iceberg melting was divided into four parts: surface melting from solar radiation, partial melting underwater caused by buoyancy vertical convection and forced convection, wave erosion at the edge, and small part of iceberg cracking [6,8,28]. As the surface melting is relatively small compared with other items, the parameterization of iceberg melting includes three key elements: bottom melting, lateral melting, and wave erosion [27]. According to the Submarine Melt Rate (SMR) formula for the melting rate of underwater ice of icebergs adopted by Fitzmaurice et al. [16]:

$$SMR = \frac{dW}{\rho_i A_{ave} dT} \tag{1}$$

where dW is the change in ice mass over a certain period of time, ρ_i is the density of the ice, A_{ave} is the average immersed total surface area of the ice, and dT is the time when the ice melts. The formula is used to calculate the side melting rate and the bottom melting rate, respectively, which is conducive to study of the ice bottom and side melting rates under the experiment.

In order to study the interaction between ice melting and flow field under distinct flow velocity, the turbulent energy dissipation rate and shear effect in each region around the ice were measured by the PIV system.

Turbulent energy dissipation rate ε is defined as:

$$\varepsilon = 2vS_{ij}S_{ij} = v\frac{\partial u_i}{\partial x_j}\left(\frac{\partial u_i}{\partial x_j} + \frac{\partial u_j}{\partial x_i}\right) \tag{2}$$

where $v = 1.335 \times 10^{-6}\ \mathrm{m^2/s}$ is the kinematic viscosity coefficient, S_{ij} is the strain rate tensor, double indices indicate summation over all three directions, and $\frac{\partial u_i}{\partial x_j}$ is the velocity gradient. Using planar PIV we can measure the terms of two dimensions in Equation (2) directly.

According to the definition of turbulent energy dissipation rate and the fluid continuity equation, Formula (2) is derived as the two-dimensional turbulent dissipation rate ε_D under the assumption of incompressibility and isotropy of the fluid [29]:

$$\varepsilon_D = 2v\left[\left(\frac{\partial u}{\partial x}\right)^2 + \left(\frac{\partial w}{\partial z}\right)^2 + \left(\frac{\partial u}{\partial z}\right)^2 + \left(\frac{\partial w}{\partial x}\right)^2 + 2\left(\frac{\partial u}{\partial z}\frac{\partial w}{\partial x}\right) + \frac{2}{3}\left(\frac{\partial u}{\partial x}\frac{\partial w}{\partial z}\right)\right] \tag{3}$$

4. Data Analysis

4.1. Melting Rate of Ice under Waves

By calculating the bottom and side melting rate under distinct waves according to Formula (1), the ice melting process was analyzed. From the experimental results of groups

1 to 5, it can be seen that the ambient temperature, water temperature, and wave elements all have certain effects on the side and bottom melting of ice block (Table 2).

Table 2. Side SMR and Bottom SMR of ice cube.

Experimental Group Number	1	2	3	4	5
Side SMR (cm/min)	0.146	0.011	0.084	0.133	0.055
Bottom SMR (cm/min)	0.124	0.009	0.074	0.110	0.044

In the experiment, two groups of ice samples (group 1 and group 2) were subjected to the same ambient and water temperature conditions, except that group 1 was exposed to wave effects while group 2 was not. It can be seen that the SMR of group 1 was significantly higher than that of group 2 (more than 10 times), which means that waves played a more significant role in this process than temperature. Under the conditions of the same water temperature and similar wave height, the difference in SMR was not significant due to different ambient temperatures between the group 1 and group 4. Therefore, the ambient temperature is not the main factor affecting ice melting. Under the same ambient temperature and similar wave height conditions, the SMR of group 4 with higher water temperature (2.4 °C) was significantly higher than that of group 5 with lower water temperature (1.0 °C), which can also be shown for group 1 and group 5. Wave and water temperature play a significant role in the process of ice melting. In order to better analyze the impact of waves on ice melting, the following analysis was conducted.

The rate of the ice mass change (Rm) is described as the relative mass change during ice melting. $Rm = \frac{m_1 - m_2}{m_1}$, where, m_1 is ice mass at the beginning of the experiment, while m_2 is ice mass at a certain moment during the melting process (Figure 3). Through controlled experiments with and without waves, the effect of wave height on ice melting can be analyzed. When there is no wave, Rm changes linearly with time (group 7, 9, and 11), and the rate of change is very small, about 0.008/min. The Rm of the experimental group with waves (group 6, group 8, and group 10) was significantly greater than that without waves (group 7, group 9, and group 11) under the same room temperature and water temperature conditions. When there are waves, the Rm curve did not change linearly, which changed the fastest in the first 5 min of the experiment and gradually slowed down over time. This is because in the early stages of the experiment, the contact area between ice and water is relatively large, and the impact of waves on ice melting is significant. As the volume of ice decreases, the contact area between ice and water decreases, and Rm decreases too. However, in the experiment, the principle of larger wave height and larger Rm was not strictly followed. The more special one is group 10, which had the highest wave height, but Rm was not the largest. This is related to thermodynamics. When there was no wave and the air temperature was higher than water temperature, the smaller the difference between air and water temperature, the smaller Rm (group 9, group 11, and group 7). In groups 10, 11, and 12, the air temperature was lower than the water temperature, so the changes in Rm were more complex. However, it can still be found that the Rm of group 10 with the greater wave height was larger than that of group 12. The melting of ice is influenced by both thermal and dynamic processes, and the specific mechanism of these effects requires more experimental and numerical simulation research (Figure 3).

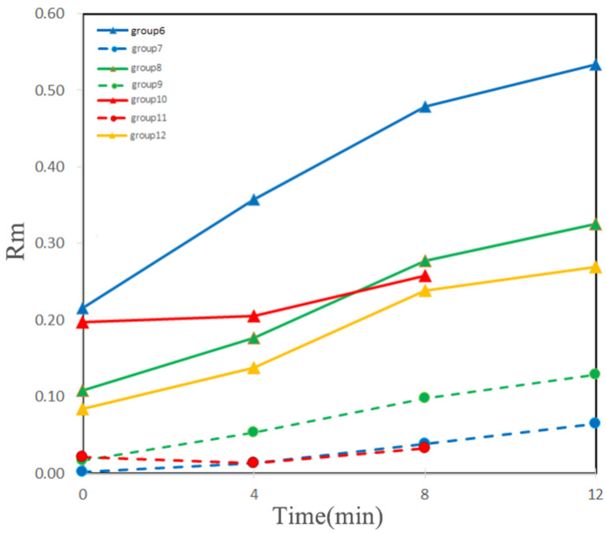

Figure 3. Time series of *Rm* at distinct wave periods.

4.2. Melting Process of Ice under Distinct Current

4.2.1. Side and Bottom Melting Rate

The Reynolds number of the side and bottom melting rate at distinct flow velocity reflects the different properties of the background flow, $\boldsymbol{Re} = \frac{\boldsymbol{UL}}{\boldsymbol{v}}$, where U is the flow speed of the background flow, and L is the width of the ice, and v Is the kinematic viscosity coefficient. In the experimental velocity range, the Reynolds number changes from 3000 to 10,000. That is, there is a transition from laminar to turbulent flow in this process. Therefore, this paper defines 0.02−0.03 m/s as the low velocity range (in the area a), in which the background flow is mainly laminar flow; 0.04−0.055 m/s is the high velocity range (in the area c), in which the background flow is mainly turbulent; and 0.03−0.04 m/s is the transition region (in the area b) (Figure 4).

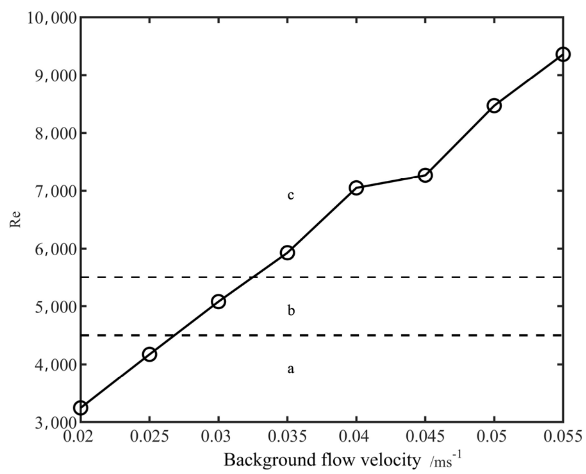

Figure 4. Reynolds number at different flow velocities.

By calculating the bottom and side melting rate using Formula (1) for ice melt, we can analyze the melting process. At the beginning of melting, the bottom melting rates are relatively close under the distinct background flow. While the bottom melting rates of low flow velocity (0.02−0.03 m/s) and high flow velocity (0.04−0.055 m/s) begin to present different characteristics over time (Figure 5). At low velocity, the ice bottom melting rate increases slowly, while it is opposite at a high flow rate where the ice bottom melting accelerates. The time-varying of the side melting rate is different from that of the bottom melting rate (Figure 6). The side melting rates increase during the melting process and are not significantly sensitive to the velocity of background flow. However, the differences still exist. The side melting rate at low velocity range (0.2−0.25 m/s) changes more slowly with time than that at a high velocity range (0.04−0.055 m/s). With the acceleration of background flow, the side melting of ice increases. Comparing the bottom and side melting rates under distinct background flow velocity, it is indicated that the bottom melting rate is more sensitive to the change of flow rate. The magnitude of SMR measured in this paper is equal to that calculated by FitzMaurice et al. [16].

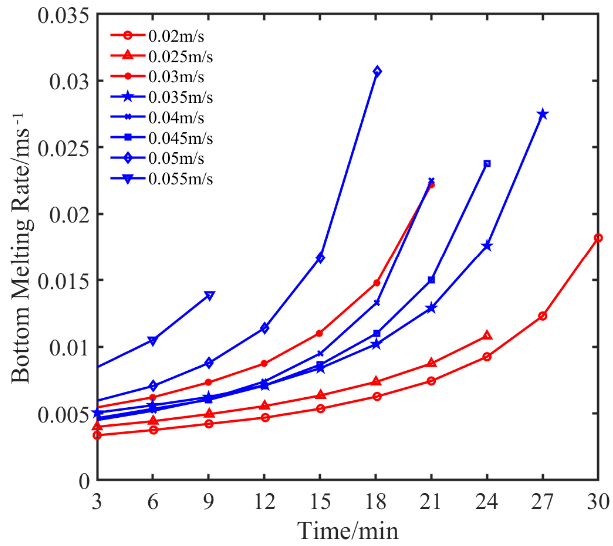

Figure 5. Time series of the bottom melting rate at diverse velocity.

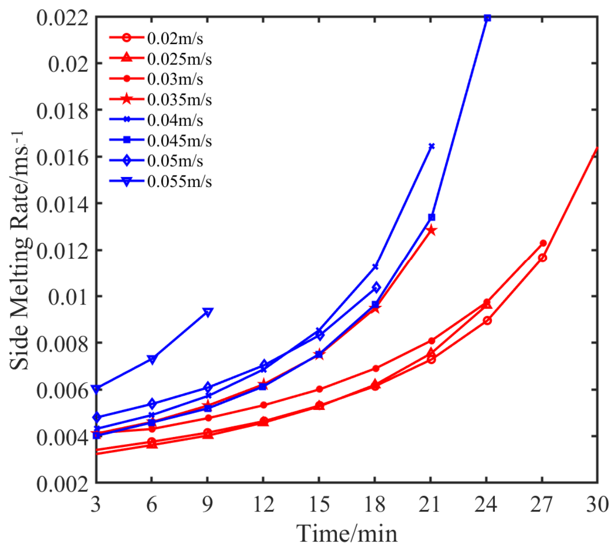

Figure 6. Time series of the side melting rate at diverse velocity.

Figure 7 presents the ratio of the bottom and side melting rates under a distinct background flow velocity. At a low velocity range, the ratio is close, while the bottom melting rate is dominant at a high velocity range (0.03−0.055 m/s), which means the ice melts more fiercely at the bottom than the side at high flow rates. Under each velocity of background flow, the proportion of side melting rate increases with time, indicating that even if the original bottom area of ice is similar to the side area, the side melting rate will dominate in the later period of melting. The side melting still plays an important role in the melting process of ice.

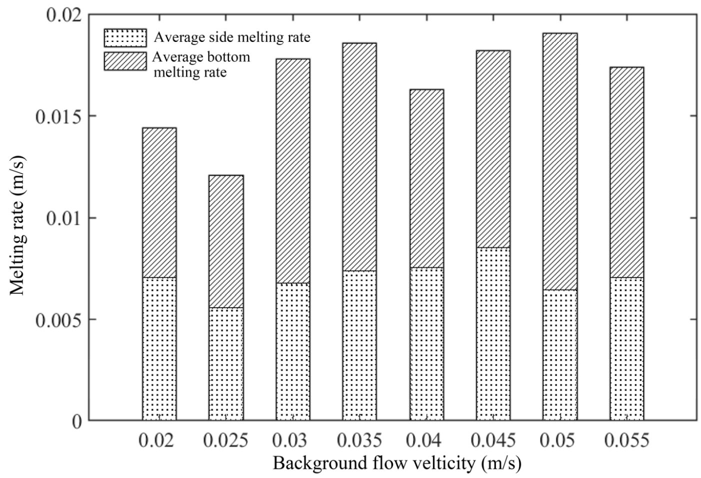

Figure 7. The ratio of the bottom melting rate and flank melting rate at diverse velocities.

Now, considering the influence of the thermal effect on the side melting of ice, the side melting heat rate *Ms* formula is often used:

$$Ms = K|\vec{u} - \vec{u}_0|^{0.8}\frac{|T_0 - T|}{L^{0.2}} \tag{4}$$

where T_0 is the water temperature, T is the ice temperature, $\vec{u}$ is ice velocity, $\vec{u}_0$ is water velocity, and L is the length of ice in the direction of background flow. K is the proportional constant that can be calculated by the formula as $K = C\frac{kPr^n}{\rho_i \Gamma v^m}$, where, ρ_i is the density of ice, and Γ is the latent heat coefficient of ice [3], k = 0.563 is the thermal conductivity coefficient of water, v is the viscosity coefficient, and Pr = 13.1 is the Planck coefficient. In seawater, C = 0.37, m = 0.8, and n = 1/3 [4]. *Ms* is derived from the theory of flow past an isothermal plate [4] and mainly studies the influence of thermal factors on the ice melting process. The magnitude of *Ms* is equal to *SMR*. However, *Ms* increases linearly with the flow rates (Figure 8), which cannot reflect the difference between the high and low velocities shown in Figures 4 and 5. *Ms* shows that the velocity along the ice face can act as a strong control on the melt rate, with fast plumes inducing much more melting than slow plumes. While this parameterization does not allow for lateral flow around the ice and is perpendicular to the melt plume. It consequently does not account for the influence of a background advective velocity on melting, either directly or via the flow's interactions with melt plumes. We will focus on studying the effects of melt plumes and shear on ice melting in the following part.

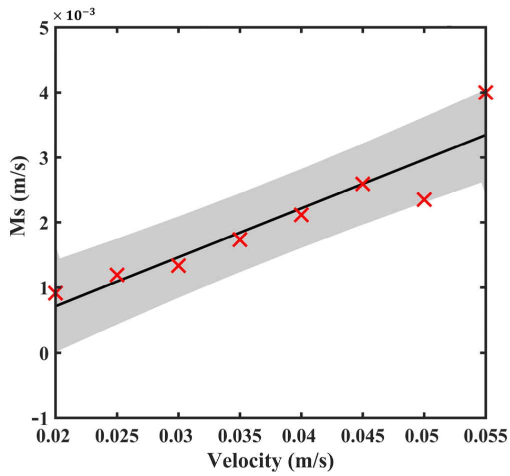

Figure 8. Ice side melting rate at diverse velocities. The black line is the linear fit line and the shading indicates 95% prediction interval.

4.2.2. Melting Plume

The dynamic mechanism of ice melting cannot be ignored at distinct background flow velocities. The ice dyeing experiment is used to track the flow of meltwater to further verify the above view. At distinct flow velocities, the melting rate of ice is related to not only the mixing of the ice melting plume and background water, but also the characteristics of meltwater. At a low velocity, the background flow is mainly laminar flow, and the meltwater plume is generated when the ice melts (Figure 9a). The meltwater has no obvious vortex structure, and the mixing depth is shallow. The meltwater around the bottom is mainly of low temperature, so the melting rate of the bottom is slow. As shown in the top view of the bottom of the ice in Figure 9b, the ice has less vortices on both sides of the downstream, and the mixing is weak. The meltwater is attached to both sides of the ice in the form of plumes. The melting rate of the side ice is slowed down by the lower temperature of the meltwater. At a high velocity, the background flow is mainly turbulent, and the surface of meltwater and ice are separated, and the mixing is enhanced. Figure 9c shows that the meltwater produced by the interaction of background flow and ice falls off in the form of a vortex, which makes the meltwater with lower temperature separate from the ice. Therefore, the ice directly contacts with the background flow with higher temperature, and the melting accelerates. The shedding of vortex is also observed on the side (Figure 9d). In addition, a large number of topographic vortices are generated in the downstream ice back region (Figure 9c). Vortices accelerate mixing and separate meltwater from ice rapidly, resulting in the difference of lateral melting rate at high velocity. Vortices accelerate mixing and melt rapidly, so the bottom and the downstream side of ice have a concave structure. The above dyeing experiments observed the distribution of the meltwater plume, which further verified the conjecture and analysis of the dynamic mechanism of ice melting under distinct background flow velocities and different regions.

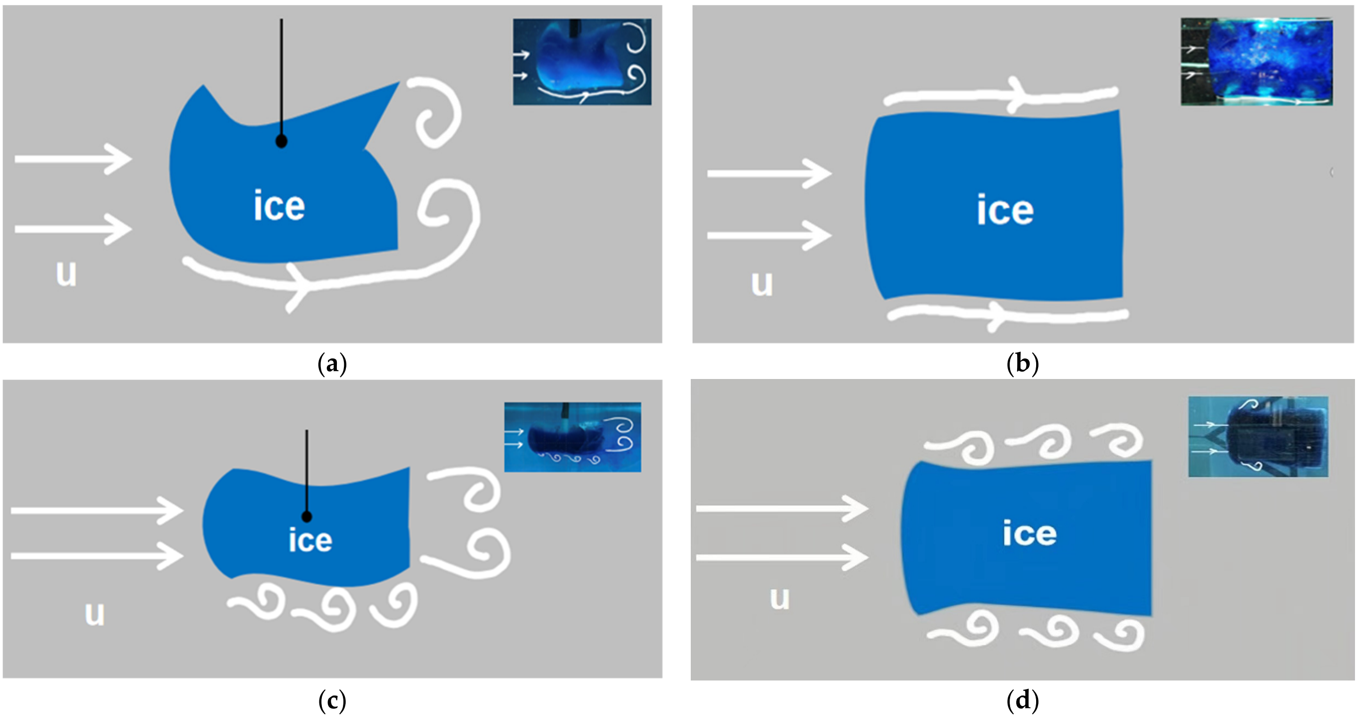

Figure 9. Side view (**a**,**c**) and top view (**b**,**d**) of ice meltwater distribution, respectively, at 0.02 m/s and 0.05 m/s flow rate.

4.2.3. Shear and Turbulent Dissipation Rates at Distinct Flow Velocity

In order to study the dynamic mechanism of ice melting at distinct flow velocities, the PIV system was used to measure the background flow distribution during ice melting at a low velocity range (0.02 m/s) and a high velocity range (0.05 m/s). The turbulent energy dissipation rate, shear, and curl inferred from the PIV system are calculated according to Formula (3). The turbulent dissipation rate is largest in the ice bottom and the ice back area in the direction of coming flow, so the experimental area was divided into the ice bottom boundary layer area and the ice back boundary layer area for research. According to Figure 10a, the turbulent energy dissipation rate at the ice bottom at high velocity is significantly higher than that at low velocity, while the turbulent energy dissipation rate at high velocity after ice is slightly higher. Figure 10b shows the shear strength under different flow velocity and areas. In the ice bottom and ice back areas, the shear strength under a high velocity range is stronger than that under a low velocity range. Therefore, the turbulent mixing caused by shear instability might be an important reason that causes the bottom melting to be faster than the side melting at high background flow velocities. In addition, the reason for the difference of ice melting under distinct flow velocity caused by the turbulent energy dissipation rate needs to be further analyzed and discussed according to the spatial distribution of the flow speed field.

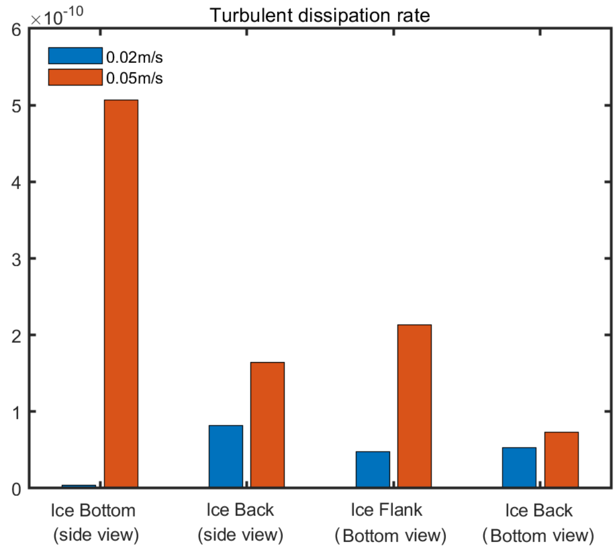

(**a**)

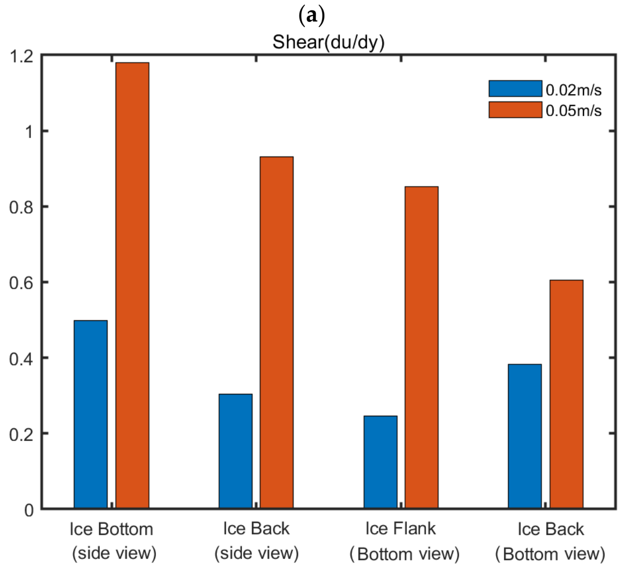

(**b**)

Figure 10. Average turbulent dissipation rate (**a**) and shear (**b**) of 0.02 m/s and 0.05 m/s velocity under different areas (including the ice bottom, the ice back, and ice flank from the side and bottom view, respectively).

For the ice bottom boundary layer area, the ice bottom is attached by a layer of fluid with weak shear, small curl, and low turbulent dissipation rate at low flow rate (Figure 11a,c,e). It is judged that this layer of fluid is the melting water with a lower temperature generated by ice melting. The adhesion of the melting water makes the ice bottom mixing weaker and the heat dissipation slower. Therefore, the heat exchange between the ice with a higher ambient temperature and the background flow is slower, so the melting of the ice bottom is slower at low background flow rate. At the high background flow velocity, Figure 11b shows that the ice bottom boundary layer shear is intense, and the turbulent energy dissipation rate is the maximum value in the ice bottom area (Figure 11d). Therefore, the meltwater with extremely strong shear instability cannot adhere to the surface of the ice. The meltwater falls off in the form of a vortex (Figure 11f), and is accompanied by violent turbulent mixing. The background flow with high ambient temperature carries out rapid heat exchange with the ice, resulting in rapid melting of the ice bottom at a high velocity range.

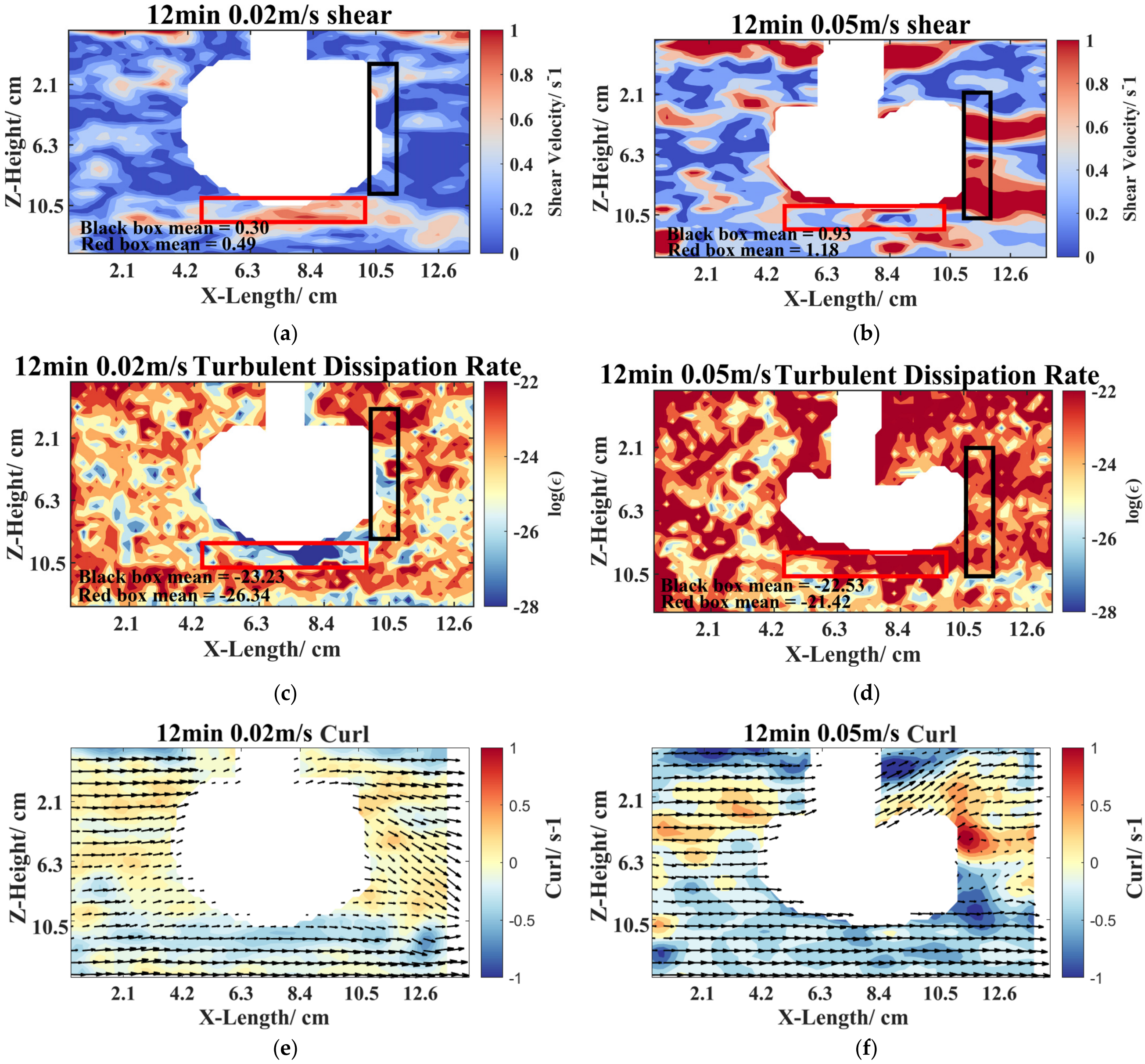

Figure 11. Shear (**a**,**b**) and turbulence dissipation rates (**c**,**d**), and curl distribution (**e**,**f**) at 0.02 m/s and 0.05 m/s flow rates. The arrows indicate the velocity field. The red (black) box is the bottom (back) of the ice selected to average.

In the ice back boundary layer, the shear is weak at a low flow rate (Figure 11a), and there is no obvious vortex shedding (Figure 11e), and the turbulent dissipation rate is relatively uniform in the whole ice back region (Figure 11c). This means that the shear instability is not the main cause of turbulent dissipation at the low flow velocity. The melted low-temperature water from the ice adheres to the ice back region and mixes with the surrounding water. As such, the convective instability is caused by the temperature difference. At high current, there is a strong flow around the ice that is symmetrical between the upper and lower behind the ice (Figure 11b). From the perspective of the curl field, it is the formation of a Carmen vortex street, with positive and negative vortices alternately separating (Figure 11f). The shedding of vortex streets leads to strong turbulent dissipation. Therefore, the turbulent dissipation caused by the terrain vortex is the reason of the ice back mixing at high flow rate.

5. Results and Discussion

Laboratory experiments indicate that waves have a significant impact on ice melting. When the wave height is almost equal to the thickness of the ice, the side and bottom melting rates of the ice are approximately several times higher than under same environment conditions without waves. The results of controlled experiments showed that the higher wave heights, the greater the melting rates. This phenomenon is due to an increase in the contact area between ice and water by waves, as well as the great turbulent dissipation by the strong mixing and shear at the ice–water interface. In the experiments of ice melting under distinct current velocity, the characteristics of ice bottom melting, ice side melting, and ice back melting were studied. The results showed that the melting of ice is significantly affected by the background flow rate, which is consistent with the previous research. However, previous empirical formula consequently do not account for the influence of background advective velocity on melting, either directly or via the flow's interactions with melt plumes. We focused on studying the effects of melt plumes and shear on ice melting in this work. The experiments showed that the ice bottom melting rate is more sensitive to the background flow velocity than the side melting rate. Meltwater is attached to the bottom in the form of plume at a low background flow velocity, while at a high background flow velocity, there is strong shear instability in the flow fields at the ice bottom and behind the ice. The dissipation and mixing effects caused by vortices accelerate the melting of the ice bottom and the ice back area.

The laboratory experiments are used to study the effects of waves and currents on ice melting, with a focus on exploring the dynamic process of ice melting. Due to the instability of air temperature and water temperature in the experiment, it is difficult to extract patterns by the complex phenomenon. As such, effectively separating the dynamic and thermodynamic processes in ice melting is needed to improve the accuracy of temperature control of experimental equipment. We will also carry out computational fluid dynamics and numerical simulation research on the ice melting.

Author Contributions: Conceptualization, X.C. and J.M.; Formal analysis, Y.C.; Funding acquisition, Y.C.; Investigation, D.T.; Methodology, T.H.; Software, H.H.; Supervision, X.L.; Writing—original draft, T.H., H.H. and D.T.; Writing—review and editing, Y.C. All authors have read and agreed to the published version of the manuscript.

Funding: This research was funded by the National Natural Science Foundation of China (Grant No. 42076228 and No. 42276239).

Informed Consent Statement: Not applicable.

Acknowledgments: We are grateful to Hanwen Bi and Yiguo Li for providing the measured data of the PIV. We would like to thank Xiao He and Jiao Tan for their friendly help.

Conflicts of Interest: The authors declare no conflict of interest.

References

1. Bamber, J.L.; Aspinall, W.P. An expert judgement assessment of future sea level rise from the ice sheets. *Nat. Clim. Chang.* **2013**, *3*, 424–427. [CrossRef]
2. Enderlin, E.; Hamilton, G.S. Estimates of iceberg submarine melting from high-resolution digital elevation models: Application to Sermilik Fjord, East Greenland. *J. Glaciol.* **2014**, *60*, 1084–1092. [CrossRef]
3. Savage, S.B. Aspects of iceberg deterioration and drift. In *LNP 582: Geomorphological Fluid Mechanics*; Balmforth, N.J., Provenzale, A., Eds.; Springer: Berlin/Heidelberg, Germany, 2001; pp. 279–318.
4. Weeks, W.F.; Campbell, W.J. Icebergs as a fresh-water source: An appraisal. *J. Glaciol.* **1973**, *12*, 207–233. [CrossRef]
5. Holland, D.M.; Jenkins, A. Modeling thermodynamic ice-ocean interactions at the base of an ice shelf. *J. Phys. Oceanogr.* **1999**, *29*, 1787–1800. [CrossRef]
6. Bigg, G.R.; Wadley, M.R.; Stevens, D.P.; Johnson, J.A. Modelling dynamics and thermodynamics of icebergs. *Cold Reg. Sci. Technol.* **1997**, *26*, 113–135. [CrossRef]
7. Stern, A.A.; Adcroft, A.; Sergienko, O.; Marques, G. Modeling tabular icebergs submerged in the ocean. *J. Adv. Model. Earth Syst.* **2017**, *9*, 1948–1972. [CrossRef]
8. Gladstone, R.M.; Bigg, G.R.; Nicholls, K.W. Iceberg trajectory modeling and meltwater injection in the Southern Ocean. *J. Geophys. Res. Atmos.* **2001**, *106*, 19903–19915. [CrossRef]
9. Josberger, E.G.; Neshyba, S. Iceberg melt-driven convection inferred from field measurements of temperature. *Ann. Glaciol.* **1980**, *1*, 113–117. [CrossRef]
10. Stephenson, G.R.; Sprintall, J.; Gille, S.T.; Vernet, M.; Helly, J.J.; Kaufmann, R.S. Subsurface melting of a free-floating antarctic iceberg. *Deep Sea Res. Part II* **2011**, *58*, 1336–1345. [CrossRef]
11. Helly, J.; Kaufmann, R.; Stephenson, G.; Vernet, M. Cooling, dilution and mixing of ocean water by free-drifting icebergs in the Weddell Sea. *Deep Sea Res.* **2010**, *58*, 1346–1363. [CrossRef]
12. Huppert, H.E.; Turner, J.S. Ice blocks melting into a salinity gradient. *J. Fluid Mech.* **1980**, *100*, 367–384. [CrossRef]
13. Russell-Head, D. The melting of free-drifting icebergs. *Ann. Glaciol.* **1980**, *1*, 119–122. [CrossRef]
14. Gade, H.G. When ice melts in sea water: A review. *Atmos. Ocean* **1993**, *31*, 139–165. [CrossRef]
15. McConnochie, C.D.; Kerr, R.C. The turbulent wall plume from a vertically distributed source of buoyancy. *J. Fluid Mech.* **2016**, *787*, 237–253. [CrossRef]
16. Fitzmaurice, A.; Cenedese, C.; Straneo, F. Nonlinear response of iceberg side melting to ocean currents. *Geophys. Res. Lett.* **2017**, *44*, 5637–5644. [CrossRef]
17. Fitzmaurice, A.; Cenedese, C.; Straneo, F. A laboratory study of iceberg side melting in vertically sheared flows. *J. Phys. Oceanogr.* **2018**, *48*, 1367–1373. [CrossRef]
18. Ikhsan, C.; Permama, A.S.; Negara, A.S. Armor Layer Uniformity and Thickness in Stationary Conditions with Steady Uniform Flow. *Civ. Eng. J.* **2022**, *8*, 1086–1099. [CrossRef]
19. Chomba, I.C.; Banda, K.E.; Winsemius, H.C.; Eunice, M.; Sichingabula, H.M.; Nyambe, I.A. Integrated Hydrologic-Hydrodynamic Inundation Modeling in a Groundwater Dependent Tropical Floodplain. *J. Hum. Earth Future* **2022**, *3*, 237–246. [CrossRef]
20. Xin, L.; Yue, Z.; Qi, D. Research progress on the changes of hydrological characteristics in the Arctic waters. *Meteorol. Hydrol. Mar. Instrum.* **2022**, *39*, 39–44.
21. Chen, P.; Zhao, J. Impacts of surface wind on regional and integrated changes of sea ice in the Arctic. *Period. Ocean. Univ. China* **2017**, *47*, 1–12.
22. Ni, B.; Zeng, L.; Xiong, H.; Wu, Q. Review on the interaction between sea ice and waves/currents. *Chin. J. Theor. Appl. Mech.* **2021**, *53*, 641–654. [CrossRef]
23. Adrian, R.J. Particle-Imaging Techniques for Experimental Fluid-Mechanics. *Annu. Rev. Fluid Mech.* **1991**, *23*, 261–304. [CrossRef]
24. Tropea, C.; Yarin, A.; Foss, J. (Eds.) *Handbook of Experimental Fluid Mechanics*; Springer: New York, NY, USA, 2007.
25. Wereley, S.T.; Meinhart, C.D. Recent Advances in Micro-Particle Image Velocimetry. *Annu. Rev. Fluid Mech.* **2010**, *42*, 557–576. [CrossRef]
26. Katz, J.; Sheng, J. Applications of Holography in Fluid Mechanics and Particle Dynamics. *Annu. Rev. Fluid Mech.* **2010**, *42*, 531–555. [CrossRef]
27. Westerweel, J.; Elsinga, G.E.; Adrian, R.J. Particle Image Velocimetry for Complex and Turbulent Flows. *Annu. Rev. Fluid Mech.* **2013**, *45*, 409. [CrossRef]
28. Martin, T.; Adcroft, A. Parameterizing the fresh-water flux from land ice to ocean with interactive icebergs in a coupled climate model. *Ocean. Model.* **2010**, *34*, 111–124. [CrossRef]
29. Doron, P.; Bertuccioli, L.; Katz, J. Turbulence Characteristics and Dissipation Estimates in the Coastal Ocean Bottom Boundary Layer from PIV Data. *J. Phys. Oceanogr.* **2001**, *31*, 2108–2134. [CrossRef]